

Bimetallic Ag–Ru/ γ -Al₂O₃ nanoparticles for selective hydrogenation of cinnamaldehyde to hydrocinnamaldehyde

Rongrong Li¹ ✉, Hong Chen¹, Zhixing Gan², Ming Jiang³, Aiguo Zhong¹, Huanhuan Bao³

¹School of Pharmaceutical and Chemical Engineering, Taizhou University, Linhai, Zhejiang, 317000, People's Republic of China

²Key Laboratory of Optoelectronic Technology of Jiangsu Province, School of Physical Science and Technology, Nanjing Normal University, Nanjing 210023, People's Republic of China

³School of Life and Science, Taizhou University, Linhai, Zhejiang, 317000, People's Republic of China

✉ E-mail: lrr@tztc.edu.cn

Published in Micro & Nano Letters; Received on 12th June 2017; Revised on 28th August 2017; Accepted on 25th October 2017

This work reports an efficient co-catalyst of AgRu nanoparticles supported on γ -Al₂O₃ for highly selective hydrogenation of the C=C bond of cinnamaldehyde (CAL) at 443 K, uncovering a catalytic route for selective hydrocinnamaldehyde production from the CAL. This kind of chemo-selectivity of AgRu/ γ -Al₂O₃ catalyst seems unique since any competitive hydrogenation at the conjugated C=O bond was significant.

1. Introduction: Supported Ag catalysts are widely used in oxidation [1, 2] and reduction reactions [3–5]. In recent years, Ag was used in the catalytic reduction in the hydrogenation of α , β -unsaturated aldehydes or ketones, which was in favour of the hydrogenation at the C=O bond [6–11].

Different metals have different selectivity in hydrogenation of C=C and C=O. For instance, platinum and palladium are the most active metals that can be used in cinnamaldehyde (CAL) selective hydrogenation reactions [12]. Mahoney [13] used [(Ph₃P)CuH]₆ for reduction of C=C and C=O selective hydrogenation reactions. The reaction proceeds at room temperature and is highly regioselective, affording either the product of conjugate reduction or complete 1,4- and 1,2-reduction to the saturated alcohol. Lipshutz [14] used base metals from groups 10 and 11 like Ni and Cu for homogeneous and heterogeneous catalysis in C=C and C=O selectivity reaction which used silanes or boranes as reducing agents. (pyr)₂Co(CH₂SiMe₃)₂ was used in cobalt-catalysed homogeneous hydrogenation for C=C, C=O, and C=N bonds [15]. Moreover, ZrO₂, Al₂O₃ and SiO₂ were used as supports for hydrogenation of CAL [16, 17]. Platinum and rhodium particles encapsulated in Y-type zeolite are much more selective for the hydrogenation of CAL to cinnamyl alcohol (COL) than active charcoal-supported platinum and rhodium catalysts [18].

The selective hydrogenation of unsaturated aldehydes to the corresponding alcohols by silver catalysts supported on metal oxides showed moderate performance both in activity and selectivity [19–21]. Compared with the conventional hydrogenation metals like Pd, Ru or Rh, Ag catalysts have unusual hydrogenation properties since the adsorption properties of silver towards the conjugated double bond. Acrolein and allyl alcohol, detected by High resolution electron energy loss spectroscopy (HREELS) and Temperature programmed desorption (TPD) [22], have a strong interaction on silver surfaces. The results, detected by Near Edge X-ray absorption fine structure (NEXAFS) and Temperature-programmed reaction spectrometry (TPRS) [23, 24], showed a bifunctional bonding on Ag, which is between the C=C group and a surface-bound oxygen, resulting in the formation of an allyloxy (2-propenyloxy) intermediate. Such surface species could well act as a precursor for the unsaturated alcohol during the hydrogenation of α , β -unsaturated aldehydes. The selectivity to unsaturated alcohol in gas phase hydrogenation of α , β -unsaturated aldehydes is higher. Thus, the low heat of adsorption of hydrogen is another common feature between silver and bimetallic catalysts. In addition

to a suitable sorption structure of the α , β -unsaturated aldehyde, it could be necessary to hydrogenate preferentially the C=O group because strongly adsorbed hydrogen reacts more readily with the C=C group than weakly adsorbed hydrogen [25]. Meanwhile, hydrocinnamaldehyde (HCAL) from the hydrogenation of the conjugated C=C bond was an important intermediate which was used for the synthesis of pharmaceuticals for the treatment of HIV [26].

Recently, we synthesised Ag/ γ -Al₂O₃ catalysts modified with Ru in the liquid-phase hydrogenation of CAL, and characterised by X-ray diffraction (XRD), X-ray photoelectron spectroscopy (XPS), transmission electron microscopy (TEM), elemental mapping and Fourier-transform infrared (FT-IR). In contrast to earlier documentations in which COL was the favourable product over supported silver catalysts [19–21], for the first time, we show that Ru, as an efficient co-catalyst of Ag/ γ -Al₂O₃, presents an unusual selectivity for the production of HCAL in the hydrogenation of CAL. This Letter might give us a new design for the development of supported silver catalysts and the modified Ag–M bimetallic catalysts.

2. Experimental: Ru-modified Ag/ γ -Al₂O₃ catalysts can be prepared by the ammonia-evaporation deposition–precipitation method. A typical procedure is presented as follows. The Ag loading is 8 wt% and the mole loading of Ru is from 1:0.1 to 1:0.02 (the molar ratio of Ag/Ru). A certain amount of AgNO₃ was dissolved in 50 ml of deionised water. 5 mL of 28 wt% ammonia aqueous solution was added and stirred for 60 min at 303 K to form a silver ammonia complex solution. Then 5 ml aqueous solution which contains a certain amount of RuCl₃·2H₂O was added into the solution and stirred for another 60 min at 303 K. Then a certain amount of γ -Al₂O₃ was added to the above silver ammonia complex solution and stirred for another 4 h at 303 K. The initial pH of the suspension was 11–12. The suspension was then preheated at 363 K to allow the evaporation of ammonia and the decrease of pH and the deposition of silver species on silica consequently. When the pH value of the suspension was decreased to 7.0, the evaporation process was over. The filtrate was washed with deionised water three times and ethanol once and then dried at 383 K overnight. Then the precursors were calcined at 673 K for 4 h, and the reduction was performed at 673 K for 4 h with a ramping rate of 2 K min^{−1} under a H₂ atmosphere. The catalyst was denoted as AgRux/ γ -Al₂O₃, where *x* stands for the molar ratio of Ru/Ag.

Table 1 Catalytic performance of catalysts with different Ag and Ru loadings for CAL hydrogenation^a

Entry	Catalyst	BET surface area, m ² /g	Absolute errors of S_{BET}	Results of Inductively coupled plasma (ICP)			Conversion, %	Selectivity, %			
				Ag, mg/kg	Ru, mg/kg	Ru/Ag ratio		HCAL	HCOL	COL	Others
1	AgRu0.1/Al ₂ O ₃ ^b	202.9	0.2	7186	1006	0.14	14.4	80.1	17.3	2.1	0.5
2	AgRu0.08/Al ₂ O ₃	224.4	−0.5	7245	797	0.11	34.1	89.1	8.7	1.6	0.6
3	AgRu0.04/Al ₂ O ₃	238.3	0.2	6985	314	0.045	93.4	94.3	0.6	3.8	1.3
4	AgRu0.02/Al ₂ O ₃	197.8	0.3	7221	209	0.029	31.4	78.8	16.5	3.9	0.8
5	Ag/Al ₂ O ₃ ^b	183.8	0.1	7021	—	—	47.5	38.4	5.9	55.2	0.5
6	Ru/Al ₂ O ₃	190.7	−0.4	—	995	—	9.7	39.4	41.8	18.5	0.3
7	Al ₂ O ₃	240.1	−0.1	—	—	—	0	—	—	—	—

^aReaction conditions: 0.2 g catalyst, 0.1 ml CAL, 30 ml cyclohexane, time = 3 h, p(H₂) = 3.0 MPa, temperature = 443 K, stirring rate = 1000 rpm.^bAg loading = 8 wt%.^cMole loading of Ru is the same as that in catalyst AgRu0.1/Al₂O₃.

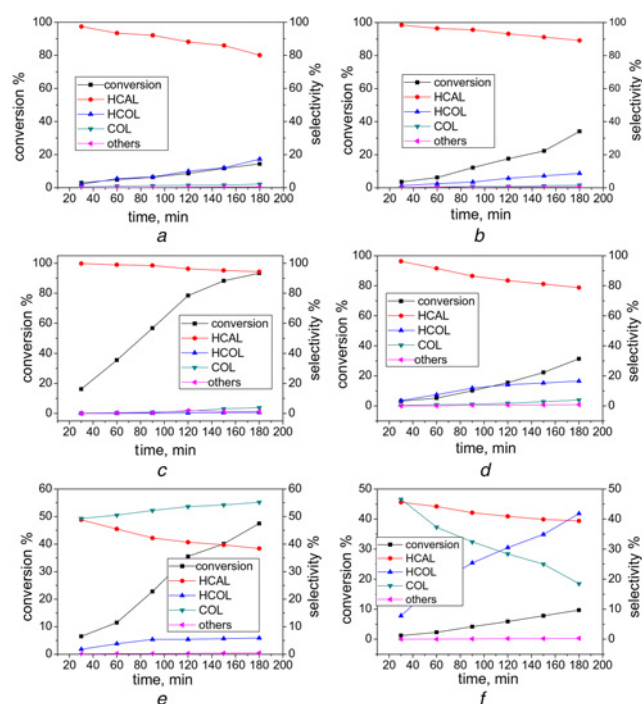
Brunauer–Emmett–Teller (BET) measurements of the solid materials were carried out with nitrogen adsorption at 77 K on a Micromeritics ASAP 2010C instrument; pre-treatments of the solid materials were carried out by degassing at 383 K for 2 h. The metal loading content of the nanocatalyst was determined by inductively coupled plasma atomic emission spectroscopy (Perkin Elmer Optima 3000DV). TEM and energy dispersive X-ray spectroscopy (EDX) study was carried out using a Philips-FEI Tecnai G2 F30 S-Twin instrument. XRD measurements of the catalyst samples were performed on a PANalytical-X'Pert PRO diffractometer. FT-IR spectra of the microsphere samples were recorded on a Perkin-Elmer FT-IR spectrometer (IRAffinity-1, Shimadzu Co., Japan). The tested samples were prepared by the KBr-disk method. XPS was performed using a Kratos AXIS Ultra DLD spectrometer. XPS analysis was performed using the monochromatised aluminium X-ray source and pass energy of the electron analyser of 40 eV.

Liquid phase hydrogenation of CAL was conducted under the following conditions: 30 ml of cyclohexane, 0.1 ml of CAL and 0.2 g of the catalyst were mixed in a 50 ml steel autoclave. Air in the autoclave was purged by hydrogen, and then the reaction proceeded at the required temperature (443 K) and at 3 MPa of 99.99% pure hydrogen. n-Nonane was used as an internal standard to calibrate the reaction products. The selectivity of the hydrogenation of HCAL was calculated using the following equation:

$$S_{\text{HCAL}} = \frac{m_{\text{HCAL}}\%}{m_{\text{COL}}\% + m_{\text{HCAL}}\% + m_{\text{HCOL}}\%} \times 100\%,$$

where m_{HCAL} , m_{COL} and m_{HCOL} represent the moles of HCAL, COL and hydrocinnamyl alcohol (HCOL) in the mixture.

3. Results and discussion: The BET surface area data of the catalyst are listed in Table 1. The data of conversion and selectivity by using the catalyst of AgRu0.1/Al₂O₃ (a), AgRu0.08/Al₂O₃ (b), AgRu0.04/Al₂O₃ (c), AgRu0.02/Al₂O₃ (d), Ag/Al₂O₃ (e) and Ru/Al₂O₃ (f) were added in the supporting information (Fig. 1). The BET surface area of AgRu/γ-Al₂O₃ was around 200 m² g^{−1}. However, when Ag/Ru = 1/0.04, With the addition of Ru, the BET surface area was decreased from 240.1 to 190.7 m² g^{−1} (Ru/Al₂O₃), but when the catalyst was the AgRu bimetallic system, the specific surface area was increased on the contrary of the amount of Ru (Ag/Ru from 0.1 to 0.04) introduced, and decreased to Ag/Ru = 0.02. The TEM images of monometallic as well as bimetallic catalysts and the corresponding particle size distributions are displayed in Fig. 2. The elemental mapping analysis of AgRu nanoparticles (AgRuNPs) was performed within a random area (Fig. 3). Fig. 2 shows that Ag/Al₂O₃ seems agglomerated. When the Ru was

**Fig. 1** Data of conversion and selectivity by using the catalysta AgRu0.1/Al₂O₃b AgRu0.08/Al₂O₃c AgRu0.04/Al₂O₃d AgRu0.02/Al₂O₃e Ag/Al₂O₃f Ru/Al₂O₃

added into Ag/Al₂O₃, the mean particle sizes were smaller than Ag/Al₂O₃. The mean particle sizes of Ru/Al₂O₃ were the smallest since the loading was quite low but there were still the agglomerated particles. As indicated in Fig. 2, the size of AgRu particles was distributed mainly in the range of 2.5–4.5 nm with an average size of AgRuNPs being about 3.5 nm. XPS measurements were performed on AgRu0.04/Al₂O₃ catalysts to determine the surface, near-surface composition and surface states of various species. According to the survey scan spectrum in Fig. 4a, we could observe the signals of O, Al and Ag elements. The XPS spectra of the Ag 3d and Ru 3d are presented in Figs. 4b and c, respectively. No obvious peaks of Ru were found in Fig. 4c since the amount of Ru loading was too small. It can be clearly seen from Fig. 4b that the signals of Ag 3d are composed of doublet peaks at 367.4 and 373.7 eV, corresponding to Ag 3d_{5/2} and Ag 3d_{3/2} [27], respectively, which exhibit

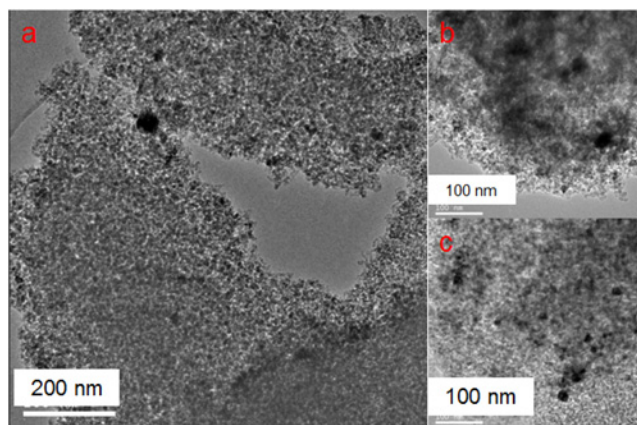


Fig. 2 TEM images
a AgRu0.04/Al₂O₃ catalyst
b Ag/Al₂O₃ catalyst
c Ru/Al₂O₃ catalyst

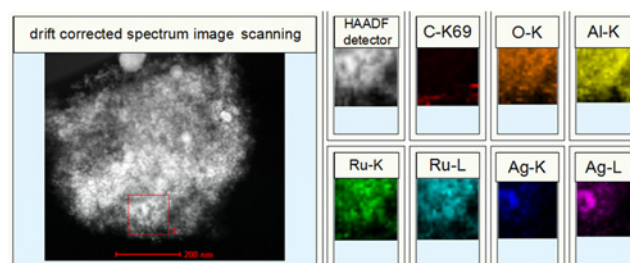


Fig. 3 Mapping EDX intensity profiles of AgRu0.04/Al₂O₃

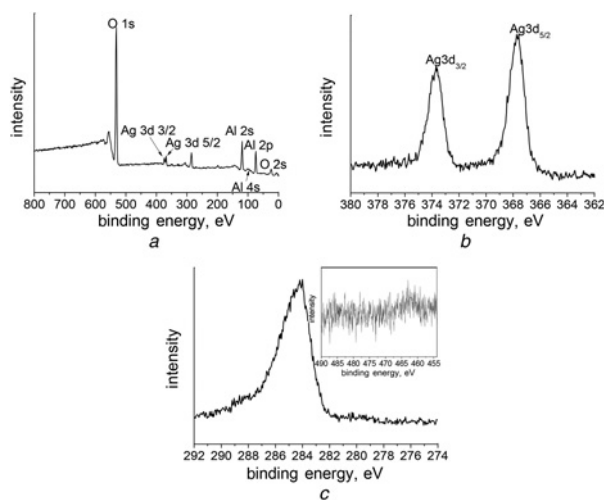


Fig. 4 XPS of fully scanned spectra
a Ag 3d
b Ru 3d
c AgRu0.04/Al₂O₃

no obvious shift in comparison with those of bulk Ag. In the XRD patterns shown in Fig. 5, the obvious crystal planes of the γ -Al₂O₃ were observed for Ag/ γ -Al₂O₃, Ru/ γ -Al₂O₃ and AgRu/ γ -Al₂O₃ samples. The peaks at $2\theta = 38.12^\circ$, 44.31° , 64.45° and 77.41° are corresponding to the (1 1 1), (2 0 0), (2 2 0) and (3 1 1) planes of gold nanoparticles (AgNPs), respectively. Meanwhile, the AgRu/ γ -Al₂O₃ catalysts had sharper peaks than the Ru/ γ -Al₂O₃ and Ag/ γ -Al₂O₃ catalysts, indicating that AgRuNPs had larger particle sizes than RuNPs or AgNPs. With the same loading,

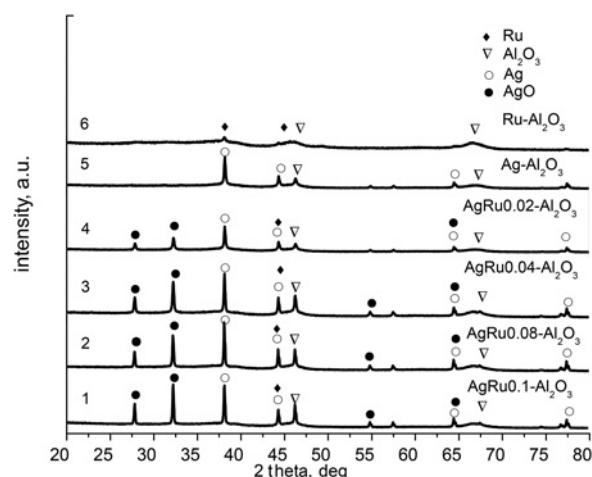


Fig. 5 XRD pattern of AgRu/ γ -Al₂O₃

Ag–Ru catalyst showed a strong diffraction peak of AgO. However, Ag catalyst did not show the diffraction peak of AgO since hydrogen may spill-over to the Ag from Ru [28].

When the hydrogenation of CAL carried out in organic solvents, several intermediates were frequently produced and accumulated during the reaction [29–31]. In Table 1, a remarkable feature of the immobilised AgRuNPs on γ -Al₂O₃ for the hydrogenation of CAL is their high selectivity for the product of HCAL, which is hydrogenation of the C=C bond. AgRu/ γ -Al₂O₃ catalyst containing the small AgRuNPs showed the high selectivity for HCAL. In comparison, AgRu0.04/Al₂O₃ catalyst had a considerable selectivity (94.4%) for the formation of HCAL at the conversion of 93.4%, when the selectivity was 95.3% at the conversion of 83.0% which used the Polyvinyl alcohol (PVA)-stabilised AgNPs on SiO₂ [32]. The products of HCAL and HCOL were about 95% of total products over the present AgRu0.04/Al₂O₃ catalysts, the by-products including 1- and 2-propyl benzenes may cause overhydrogenation and then intramolecular dehydration and any of the unidentified products were <2%. While the conversion levels of CAL over the three kinds of AgRu/Al₂O₃, Ag/Al₂O₃ and Ru/Al₂O₃ catalysts were remarkably different in Table 1. Narayan's group had studied the hydrogen adsorption states on silica-supported Ru–Ag and Ru–Cu bimetallic catalysts [28]. On Ru–Ag, the only surface metal which can adsorb hydrogen is Ru since hydrogen spilled to the Ag from Ru. The addition of Ag to Ru significantly reduced the total amount of hydrogen adsorbed per surface Ru atom. Ag preferentially occupies the low coordination metal sites. The loss of the intermediate and low adsorption energy sites is correlated with the replacement of Ru atoms at edge, corner and other defect sites by Ag. Accordingly, the C=O group has weaker adsorbed defect sites than the C=C group in the hydrogenation of CAL, the HCAL selectivity over this Ag/Al₂O₃ or Ru/Al₂O₃ catalyst was lower than that of the AgRu/Al₂O₃ catalyst. Meanwhile, the addition of Ru may improve the adsorbed hydrogen and spill-over to the Ag, while AgRu0.04/Al₂O₃ reached the highest conversion and selectivity.

To confirm the above result, FT-IR studies on adsorption of CAL onto catalysts were performed to examine the adsorption mode for the purpose to explain the enhancements observed in selectivity. The FT-IR spectra are shown in Fig. 6. As can be seen, there are two main vibration bands within the range of 1600–1700 cm^{−1}. The band centred at 1626 cm^{−1} is assigned to conjugated C=C bond stretching vibration ($\nu_{C=C}$). The other one at 1675 cm^{−1} can be assigned to C=O bond asymmetric stretching vibration ($\nu_{C=O}$) of unsaturated aldehyde. These spectra correspond to the substrate adsorbed on the catalysts, if the CAL substrate is adsorbed on the catalyst, and the Ru-containing catalyst is more active towards

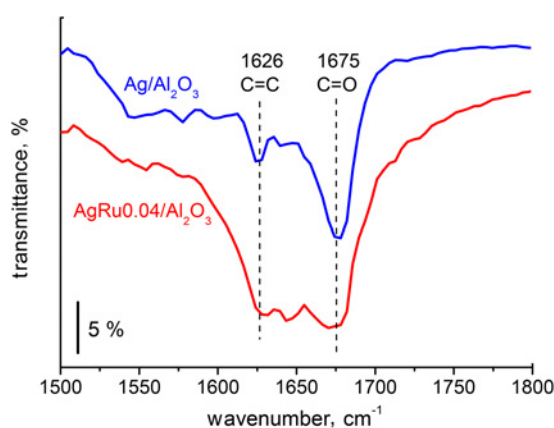


Fig. 6 FT-IR pattern of AgRu0.04/ γ -Al₂O₃ and Ag/ γ -Al₂O₃

the formation of HCAL so the C=C is prefer to adsorb onto the surface of catalysts, and the $I(\text{C}=\text{C})/I(\text{C}=\text{O})$ ratio will be higher with AgRu0.04/Al₂O₃ than with Ag/Al₂O₃. This is due to the fact that the preferential C=C adsorption modes make the phenyl ring of CAL closer to interact with the surface of catalysts [33–35]. It has been reported that gaseous CAL showed an absorption band of $\nu_{\text{C}=\text{O}}$ at 1740 cm⁻¹. Therefore, the shift of the $\nu_{\text{C}=\text{O}}$ band observed here indicated that the CAL molecules interacted with the surface of catalysts after adsorption. A more pronounced change occurred in the relative intensity ratio of the C=C to C=O absorption band ($I_{\text{C}=\text{C}}/I_{\text{C}=\text{O}}$). As shown in the FT-IR spectra of CAL adsorption in Fig. 6, with the addition of Ru, C=C bond adsorbed on Ag atoms positioned at 1626 cm⁻¹ became stronger than C=O bond adsorbed at 1675 cm⁻¹, indicating that the adsorption of the C=C bond is more favourable than that of the C=O bond in the AgRu/Al₂O₃ catalysts.

4. Conclusion: Ag/ γ -Al₂O₃ catalysts modified with Ru were synthesised and characterised by XRD, XPS, TEM, elemental mapping and FT-IR. These catalysts were used for selective hydrogenation of CAL and the conjugated C=O bond was significantly avoided with the Ru addition. From the data of FT-IR, C=C bond adsorbed on Ag atoms positioned at 1626 cm⁻¹ became stronger than the C=O bond adsorbed at 1675 cm⁻¹, indicating that the adsorption of the C=C bond is more favourable than that of the C=O bond in the AgRu/ γ -Al₂O₃ catalysts. For comparison, we synthesised the same RuNPs and AgNPs on γ -Al₂O₃ but the Ag/ γ -Al₂O₃ or Ru/ γ -Al₂O₃ catalyst affected competitive hydrogenation of both C=C and C=O bonds of the reactant CAL molecules. This different selectivity of the immobilised γ -Al₂O₃-stabilised AgRuNPs has not been reported for the hydrogenation of CAL and could enlarge the knowledge of Ag and Ru catalysts in hydrogenation.

5. Acknowledgments: This work was supported by the National Natural Science Foundation of China (grant no. 21506138) and the Natural Science Foundation of Zhejiang Province, China (grant no. LQ15B060001).

6 References

- [1] Guo D.J., Li H.L.: 'Highly dispersed Ag nanoparticles on functional MWNT surfaces for methanol oxidation in alkaline solution', *Carbon*, 2005, **43**, (6), pp. 1259–1264
- [2] Lu J.Q., Bravo-Suarez J.J.: 'In situ UV-vis studies of the effect of particle size on the epoxidation of ethylene propylene on supported silver catalysts with molecular oxygen', *J. Catal.*, 2005, **232**, (1), pp. 85–95
- [3] Tanabe K., Hattori H., Yamaguchi T., *ET AL.*: 'Function of metal oxide complex oxide catalysts for hydrocracking of coal', *Fuel Process. Technol.*, 1986, **14**, (11), pp. 247–260
- [4] Raboin L., Yano J., Tilley T.D.: 'Epoxidation catalysts derived from introduction of titanium centers onto the surface of mesoporous aluminophosphate: comparisons with analogous catalysts based on mesoporous silica', *J. Catal.*, 2012, **285**, (1), pp. 168–176
- [5] Mahata N., Goncalves F.M., Pereira F.R., *ET AL.*: 'Selective hydrogenation of cinnamaldehyde to cinnamyl alcohol over mesoporous carbon supported Fe Zn promoted Pt catalyst', *Appl. Catal. A, Gen.*, 2008, **339**, (2), pp. 159–168
- [6] Chambers A., Jackson S.D., Stirling D., *ET AL.*: 'Selective hydrogenation of cinnamaldehyde over supported copper catalysts', *J. Catal.*, 1997, **168**, (2), pp. 301–314
- [7] Durndell L.J., Parlett C.M., Hondow N.S., *ET AL.*: 'Selectivity control in Pt-catalyzed cinnamaldehyde hydrogenation', *Sci. Rep.*, 2015, **5**, pp. 9425–9434
- [8] Zhao B.H., Chen J.G., Liu X., *ET AL.*: 'Selective hydrogenation of cinnamaldehyde over Pt Pd supported on multiwalled carbon nanotubes in a CO₂-expanded alcoholic medium', *Ind. Eng. Chem. Res.*, 2012, **51**, (34), pp. 11112–11121
- [9] Zhu Y., Zera F.: 'Selectivity in the catalytic hydrogenation of cinnamaldehyde promoted by Pt/SiO₂ as a function of metal nanoparticle size', *Catal. Sci. Technol.*, 2014, **4**, (4), pp. 955–962
- [10] Piqueras C.M., Puccia V., Vega D.A., *ET AL.*: 'Selective hydrogenation of cinnamaldehyde in supercritical CO₂ over Me-CeO₂ (Me=Cu, Pt, Au): insight of the role of Me-Ce interaction', *Appl. Catal. B, Environ.*, 2016, **185**, pp. 265–271
- [11] Tian Z., Li Q., Hou J., *ET AL.*: 'Highly selective hydrogenation of α , β -unsaturated aldehydes by Pt catalysts supported on Fe-based layered double hydroxides derived mixed metal oxides', *Catal. Sci. Technol.*, 2016, **6**, (3), pp. 703–707
- [12] Merlo A.B., Vetere V., Casell M.L.: 'Silica-supported PtSn catalysts obtained through surface organometallic chemistry on metals techniques using a hydrosoluble organotin promoter. Application to the selective hydrogenation of α , β -unsaturated aldehydes ketones', *Curr. Catal.*, 2014, **3**, (2), pp. 244–253
- [13] Mahoney W.S., Stryker J.M.: 'Hydride-mediated homogeneous catalysis. Catalytic reduction of α , β -unsaturated ketones using [(Ph₃P)CuH]₆ H₂', *J. Am. Chem. Soc.*, 1989, **111**, (24), pp. 8818–8823
- [14] Deutsch C., Krause N., Lipshutz B.H.: 'ChemInform abstract: CuH-catalyzed reactions', *Cheminform*, 2008, **108**, (8), pp. 2916–2927
- [15] Zhang G., Scott B.L., Hanson S.K.: 'Mild homogeneous cobalt-catalyzed hydrogenation of C=C, C=O, C=N bonds', *Angew. Chem. Int. Ed.*, 2012, **51**, (48), pp. 12102–12106
- [16] Rojas H., Martínez J., Vargas L., *ET AL.*: 'Hidrogenación de cinamaldehyde sobre catalizadores Au/ZrO₂ y Au/ZrO₂-SiO₂. Efecto del soporte y método de preparación', *Ing. Compet.*, 2012, **14**, (2), pp. 119–124
- [17] Neri G., Mercadante L., Milone C., *ET AL.*: 'Hydrogenation of citral cinnamaldehyde over bimetallic Ru & unknown Me/Al₂O₃ catalysts', *J. Mol. Catal. A, Chem.*, 1996, **108**, (1), pp. 41–50
- [18] Gallezot P., Giroir F.A., Richard D.: 'Chemoselectivity in cinnamaldehyde hydrogenation induced by shape selectivity effects in Pt-Y zeolite catalysts', *Catal. Lett.*, 1990, **5**, (2), pp. 169–174
- [19] Claus P., Hofmeister H.: 'Electron microscopy catalytic study of silver catalysts: structure sensitivity of the hydrogenation of crotonaldehyde', *J. Phys. Chem. B*, 1999, **103**, (14), pp. 2766–2775
- [20] Grünert W., Brückner A., Hofmeister H., *ET AL.*: 'Structural properties of Ag/TiO₂ catalysts for acrolein hydrogenation', *J. Phys. Chem. B*, 2004, **108**, (18), pp. 5709–5717
- [21] Bron M., Knop-Gericke A., Teschner D., *ET AL.*: 'Bridging the pressure materials gap: in-depth characterisation reaction studies of silver-catalysed acrolein hydrogenation', *Claus, J. Catal.*, 2005, **234**, (1), pp. 37–47
- [22] Carter R., Anton A.B.: 'Reactions of π -allyl with atomic oxygen hydroxyl on Ag(110)', *Surf. Sci.*, 1993, **290**, (3), pp. 319–334
- [23] Solomon J.L., Madix R.J., Stöhr J.: ' π bonded intermediates in alcohol oxidation: orientations of allyloxy propargyloxy on Ag (110) by near edge X-ray absorption fine structure', *J. Chem. Phys.*, 1988, **89**, (8), pp. 5316–5322
- [24] Solomon J.L., Madix R.J.: 'Kinetics mechanism of the oxidation of allyl alcohol on silver(110)', *J. Phys. Chem.*, 1987, **91**, (24), pp. 6241–6244
- [25] Takeuchi T., Asano T.: 'Study of the adsorption of hydrogen the hydrogenation of ethylene on a nickel catalyst by means of tritium as tracer', *Z. Phys. Chem.*, 1963, (1–2), **36**, pp. 118–125
- [26] Muller A., Bowers J.: WO Patent Appl. 1999, No. WO 99/08989
- [27] Zhu M.Y., Wang C.J., Meng D., *ET AL.*: 'In situ synthesis of silver nanostructures on magnetic Fe₃O₄@C core-shell nanocomposites

- their application in catalytic reduction reactions', *J. Mater. Chem. A*, 2013, **1**, (6), pp. 2118–2125
- [28] Narayan R.L., King T.S.: 'Hydrogen adsorption states on silica-supported Ru–Ag Ru–Cu bimetallic catalysts investigated via microcalorimetry', *Thermochim. Acta*, 1998, **312**, (312), pp. 105–114
- [29] Milone C., Ingoglia R., Tropeano M.L., *ET AL.*: 'First example of selective hydrogenation of unconstrained α,β -unsaturated ketone to α,β -unsaturated alcohol by molecular hydrogen', *Chem. Commun.*, 2003, **34**, (30), pp. 868–869
- [30] Vannice M.A., Sen B.: 'Metal-support effects on the intramolecular selectivity of crotonaldehyde hydrogenation over platinum', *J. Catal.*, 1989, **20**, (17), pp. 65–78
- [31] Enustun B.V., Turkevich J.: 'Coagulation of colloidal gold', *J. Am. Chem. Soc.*, 1963, **85**, (21), pp. 676–687
- [32] Shi H., Zhao D., Xu B.Q.: 'Immobilized PVA-stabilized gold nanoparticles on silica show an unusual selectivity in the hydrogenation of cinnamaldehyde', *Catal. Commun.*, 2008, **9**, (10), pp. 1949–1954
- [33] Tian Z., Xiang X., Xie L., *ET AL.*: 'Liquid-phase hydrogenation of cinnamaldehyde: enhancing selectivity of supported gold catalysts by incorporation of cerium into the support', *Ind. Eng. Chem. Res.*, 2015, **52**, (1), pp. 288–296
- [34] Koutstaal C.A., Angevaere P.A.J.M., Ponc V.: 'ChemInform abstract: surface chemistry of benzoyl compounds on oxides, an FT–IR study', *J. Catal.*, 1993, **143**, (2), pp. 573–582
- [35] Zhao F., Fujita S., Akihara S., *ET AL.*: 'Hydrogenation of benzaldehyde cinnamaldehyde in compressed CO₂ medium with a Pt/C catalyst: a study on molecular interactions pressure effects', *J. Phys. Chem.*, 2005, **109**, (19), pp. 4419–4424